Available online at www.sciencedirect.com

ScienceDirect

Procedia Structural Integrity 76 (2026) 107–114

Structural Integrity Procedia

www.elsevier.com/locate/procedia

5th International Symposium on Fatigue Design and Material Defects FDMD 2025

Comparison of life prediction methods for net-shape IN718 manufactured by L-PBF

Daniel Perghem[b], Luca Patriarca[b], Lorenzo Bongiorni[a], Simone Romano[a], Stefano Beretta[b,c,*]

[a]*GE Avio s.r.l., Via Primo Maggio 99, 10040, Rivalta di Torino (TO), Italy*
[b]*Politecnico di Milano, Department of Mechanical Engineering, Via La Masa 1, 20156 Milano, Italy*
[c]*Auburn University, National Center for Additive Manufacturing Excellence (NCAME), Auburn, Al 36849, USA*

Abstract

The aerospace industry is increasingly considering metal additive manufacturing (AM) technology to produce optimized components that offer high design flexibility, complex geometries, and reduced weight. However, the surface quality and orientation of printed components remain critical factors influencing their fatigue life. This research aims to assess the impact of different surface qualities, including orientation and post-processing treatments, on the fatigue behaviour of a nickel-chromium alloy (Inconel 718) manufactured via laser powder bed fusion (L-PBF). The study examines key surface related variables that affect the fatigue strength of L-PBF parts, i.e., surface roughness and sub/near-surface anomalies, identifying the anomalies that predominantly contribute to failure across various surface qualities. A life prediction model is developed to accurately estimate fatigue life by integrating the influence of anomaly characteristics associated with specific surface treatments and orientations.

Keywords: IN718, cyclic R- curve, anomalies, fatigue strength.

1. Introduction

Additive manufacturing (AM) technologies, and in particular Laser Powder Bed Fusion (L-PBF), have enabled the fabrication of complex geometries Frazier et al. (2014). Among high-performance alloys, Inconel 718 (IN718) is widely used in aerospace and power generation due to its excellent mechanical properties at elevated temperatures Hosseini and Popovich (2019), Akca and Gürsel (2015). Nevertheless, additively manufactured (AMed) components frequently exhibit undesirable attributes, including thermal residual stresses, atypical microstructures, relatively rough surfaces, and volumetric anomalies Sanaei and Fatemi (2021), Kotadia et al. (2021). These features have been shown to significantly influence the fatigue performance of AMed parts Seifi et al. (2017).

* Corresponding author
E-mail address: stefano.beretta@polimi.it

2452-3216
10.1016/j.prostr.2025.12.293

Accurate prediction of fatigue strength in AM components remains challenging due to the presence of anomalies and variability introduced by different surface finishes and build directions Daniewicz and Shamsaei (2017), Romano et al. (2018). Several approaches have been proposed to assess the structural integrity of AMed components Yamashita et al. (2018), Beretta and Romano (2017), including the El Haddad et al. (1979) model and the R-curve based Chapetti (2003) model. While the El-Haddad model accounts for anomalie size effects on the endurance limit, its accuracy relies on the long-crack threshold, which can be determined by various experimental methods that often yield significantly different results Pippan et al. (1994). On the other hand, the cyclic R-curve by Tanaka and Akiniwa (1988) approach incorporates the growth behaviour of physically short cracks, providing a more comprehensive framework for predicting fatigue strength under variable anomalie conditions. Recent studies Madia et al. (2022), Perghem et al. (2025) indicate that the El-Haddad model can produce non-conservative predictions if non-conservative thresholds for long fatigue crack growth are used. In contrast, employing the R-curve approach has been shown to effectively overcome this limitation and provide more reliable results.

In this study, the fatigue behaviour of IN718 L-PBF specimens produced in different orientations and with different surface treatments was investigated. Experimental results from four-point bending (4PB) fatigue, single-edge bending (SEB), and micro-notched specimens were carried out and used to calibrate the El-Haddad and Chapetti models. The aim of this work is to assess the influence of build orientation and surface treatment on fatigue strength and to evaluate the capability of different fatigue strength models to predict the endurance limit of AM IN718.

Nomenclature

4PB	four-point bending
AM	additive manufacturing
CPCA	compression pre-cracking constant amplitude
CPLR	compression pre-cracking load reduction
CPDK	compression pre-cracking constant ΔK
EDM	electrical discharge machining
IN78	Inconel 718
L-PBF	laser-powder bed fusion
R	load ratio
SEB	single-edge bending
SEM	scanning electron microscope
a_{eq}	equivalent crack size
Δa	crack advancement
$\Delta K_{th,LC}$	long crack threshold range
$\Delta K_{th,LC}^{\Delta a=0}$	long crack threshold range a $\Delta a = 0$
$\Delta K_{th,LC}^{eff}$	effective long crack threshold range
$\Delta\sigma_{w,0}$	fatigue limit stress range for anomalie-free material
$\Delta\sigma_w$	fatigue limit stress range
$\sqrt{area}$	anomalie size as Murakami's parameter
$\sqrt{area}_0$	El-Haddad's parameter expressed as anomalie's projected area
Y,F	shape factor
N	number of cycles to failure

2. Material and methods

The tested specimens in IN718, as shown in Fig. 1, were produced in the Avio Aero's laboratory in Turin, using L-PBF technology. Melting process parameters for both internal volumes and external surfaces were set by the manufactured and are confidential. The specimens were produced across multiple print jobs and comprised 6 series of four-point bending (4PB) specimens, each consisting of 12 samples manufactured in different orientations with

respect to the build plate: one vertical machined series, four net-shape series (vertical, horizontal, upskin, and downskin), and one downskin series subjected to chemical milling surface treatment. In addition, single-edge bending (SEB) specimens (oriented perpendicular to the build plate) and micro-notched specimens were fabricated.

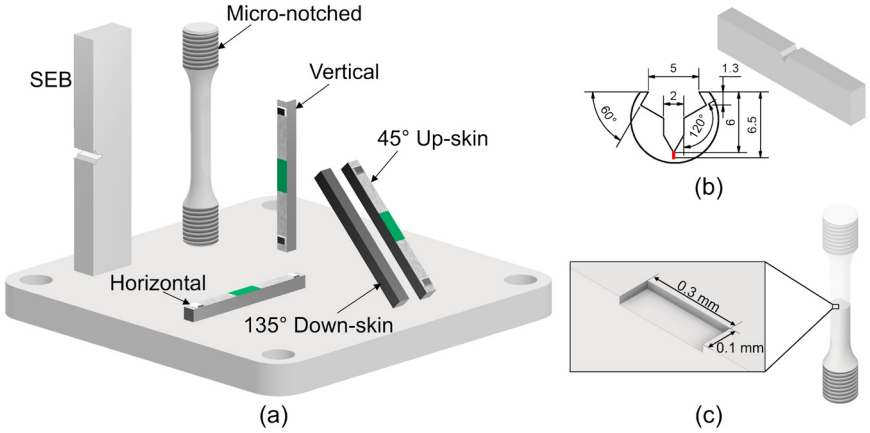

Fig. 1. (a) Geometry of the specimens tested in this study; (b) Detail of the notch geometry of Single-edge bending (SEB) specimens; (c) Detail the notch geometry of micro-notched specimens.

All 4PB fatigue tests were carried out on an MTS Acumen having a load capacity of 3 kN. The test were performed at a stress ratio R = 0.1 with a test frequency of approximately 30-35 Hz. The run-out condition was set up to 10^7 cycles, while the failure condition corresponds to a stiffness drop of 10 %. The run-outs were re-tested at the same stress ratio and at higher load levels to produce failures. After fatigue tests the 4PB specimens were broken under liquid nitrogen and the fracture surfaces were observed under a Scanning Electron Microscopy (SEM, Zeiss EVO150) to identifies the anomalies at the failure origin. Measurements of the anomaly size were taken in terms of $\sqrt{area}$ parameter proposed by Murakami (2019), the area refers to the projected surface of the anomaly on the plane perpendicular to the direction of maximum principal stress.

The SEB specimens were initially printed as parallelepiped blocks and subsequentially machined to their final shape, the notch geometry was created using electrical discharge machining (EDM), with a wire diameter of approximately 150 μm, detail of the notch is shown in Fig. 1b. Pre-cracking and crack propagation tests were performed using a Rumul resonant flexural load frame. All SEB specimen underwent pre-cracking through fatigue cycle in compression. Once the pre-cracking phase was completed, various testing methodologies were employed to measure the evolution of crack thresholds with crack length: Compression Pre-cracking Constant Amplitude (CPCA) method Pippan (1987), Compression Pre-cracking Load Reduction (CPLR) method Newman and Yamada (2010) and Compression Pre-cracking Constant-ΔK (CPDK) Pourheidar et al. (2021). More details regarding the R-curve performed at R=0.1 and -1 are reported in the work of Patriarca et al. (2024). Additionally, a set of cylindrical specimen has been machined to produced two lateral, parallel, flat surfaces and an artificial anomalies in form of tiny rectangular, with dimensions 0.1x0.3mm ($\sqrt{area} = 173\mu m$), have been carefully produced in the mid section of the specimens by EDM, as shown in Fig.1c. The micro-notched specimens were initially pre-cracked under negative load ratio and successively tested according a short staircase sequence. The pre-cracking methodology is well-documented in the literature Newman and Yamada (2010) and it effectively aims to generate an initial closure-free crack from the EDM notch.

3. Results and discussion

3.1. Fatigue test results and Analysis of fracture surfaces

The fit of the log-normal distributions was performed in accordance with ASTM E739 (2023), using the least-squares method to determine the C and b constants of the Eq.1 adopting for describe the finite-life part of the S-N

curve of each series:

$$\Delta\sigma = A \cdot N^{-b} \tag{1}$$

Hodge-Rosenblatt's up and down method with small samples and a short stair-case sequence Brownlee et al. (1953) for the fatigue limit estimation was used in the current investigation.

The results of the fatigue test at R=0.1 of the 6 series of 4PB fatigue specimens, are presented in Fig.2, normalized by the endurance limit ($\Delta\sigma_w$) of the machined series. The downskin specimens show the lowest fatigue strength, with

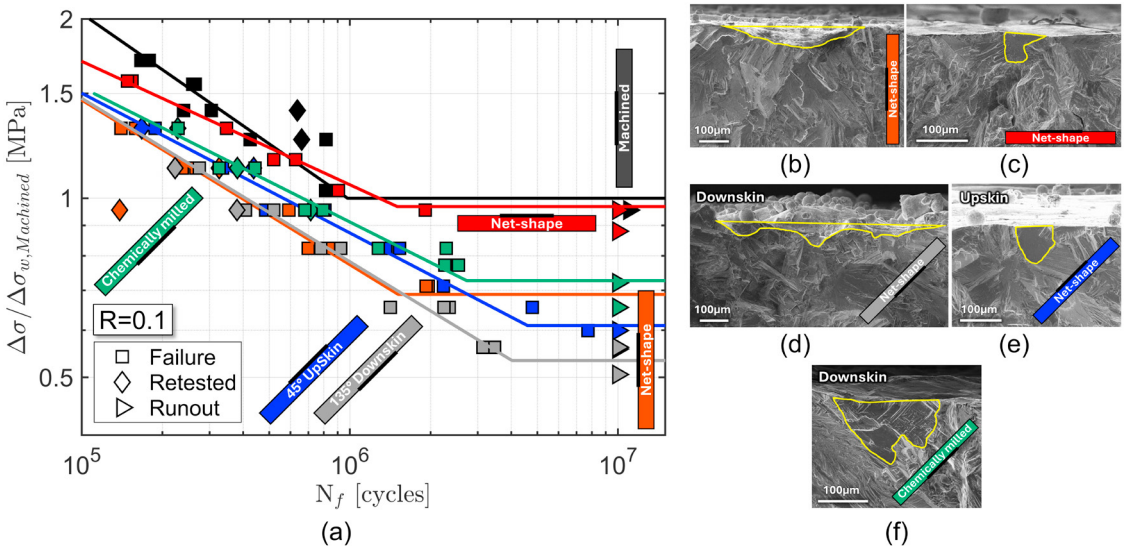

Fig. 2. (a) The results of the fatigue tests conducted at R=0.1; SEM observations of typical critical anomalies: (b) Vertical series; (c) Horizontal series; (d) Downskin series; (e) Upskin series; (f) Downskin chemically milled series.

about 55% reduction in the fatigue limit region compared to machined specimens. The horizontal specimens exhibit a fatigue limit comparable to the machined series. Surface treatment by chemical milling on the downskin surface enhances the fatigue properties. The vertical series present fatigue behaviour in the finite life region similar to the downskin condition. All series show a comparable slope in the finite life regime, which, however, differs from the one observed for the machined series.

Different types and shapes of anomalies were observed at the failure origin depending on the build orientation. High-quality surfaces, horizontal (Fig. 2c) and upskin (Fig. 2e), typically exhibited grain aggregates or intrusions, whereas rougher surfaces, vertical (Fig. 2b) and downskin (Fig. 2d), were characterized by elongated grooves. Chemical milling enhanced surface quality by eliminating rough downskin features, leading to failures originating from grain aggregates (Fig. 2f).

3.2. Fatigue strength model

3.2.1. Modelling through El-Haddad model

In this study to consider the short-crack effect for the endurance limit $\Delta\sigma_w$ the El Haddad et al. (1979) model is utilized:

$$\Delta\sigma_w = \Delta\sigma_{w,0} \cdot \sqrt{\frac{\sqrt{area}_0}{\sqrt{area} + \sqrt{area}_0}} \; with \; \sqrt{area}_0 = \frac{1}{\pi} \cdot \left(\frac{\Delta K_{th,LC}}{Y \cdot \Delta\sigma_{w,0}} \right)^2 \tag{2}$$

where $\Delta\sigma_{w,0}$ is the endurance limit stress range for anomaly-free materials, $\sqrt{area}_0$ is the El-Haddad size parameters, and $\Delta K_{th,LC}$ is the fatigue long crack propagation threshold. Based on Eq.2 the El-Haddad model requires two material parameters to be determine the $\Delta\sigma_{w,0}$ and $\Delta K_{th,LC}$.

The fatigue test results for the machined and horizontal 4PB specimens (reported as $\Delta\sigma_w$ and average $\sqrt{area}$) together with the results of the artificially micro-notched specimens, are summarized in Fig.3, which also shows the El-Haddad model using a $\Delta K_{th,LC}$ obtained through CPLR procedure. If $\Delta\sigma_{w,0}$ is quite a simple material property, one of the main challenges lies in the determination of $\Delta K_{th,LC}$. The fatigue test results indicate that the El-Haddad equation estimated with the $\Delta K_{th,LC}$-CPLR over-estimates the endurance limit of the micro-notched specimens. Therefore, a

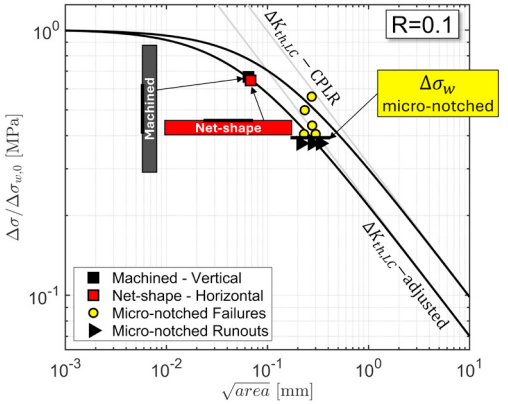

Fig. 3. El-Haddad model adopting $\Delta K_{th,LC}$-CPLR and the adjusted El-Haddad model.

different strategy was implemented to fit the Eq.2. To provide a consistent fit of the El-Haddad model, we force the El-Haddad equation to fit the endurance limits for the machined and horizontal 4PB series with their respective average $\sqrt{area}$, in addition the endurance limit for the micro-notched test was also used as an addition point in the fitting process. The results of this fitting process were the $\Delta\sigma_{w,0}$ and $\Delta K_{th,LC}$-adjusted. The new value of $\Delta K_{th,LC}$, obtained through the fitting process, is approximately 29% lower than the value experimentally determined adopting the CPLR procedure.

3.2.2. R-curve analysis

More recently, the fatigue assessment based on the cyclic R-curve has been discussed by Chapetti (2003) and Zerbst et al. (2012). The cyclic R-curve Tanaka and Akiniwa (1988) describes the increase in the fatigue crack growth threshold ΔK with crack extension Δa. This curve enables the modelling of the behaviour of physically short cracks and the analytical model used to fit the experimental data points, established by Maierhofer et al. (2014), is based on Eq.3:

$$\Delta K_{th}(R,\Delta a) = \Delta K_{th}^{\Delta a=0} + \left(\Delta K_{th,LC} - \Delta K_{th}^{\Delta a=0}\right)\cdot\left[1 - \sum_{i=1}^{n} v_i \cdot \exp\left(-\frac{\Delta a}{l_i}\right)\right] \tag{3}$$

The CPCA procedure estimates the fatigue limit by comparing the applied stress intensity factor with the cyclic R-curve. If the stress intensity range is below the R-curve, the crack arrests and does not propagate; if it exceeds the R-curve, the crack continues to grow. The fatigue limit is determined when the applied stress intensity factor becomes tangent to the cyclic R-curve. Using this concept, we can then calculate $\Delta K_{th,LC}$ for a CA procedure, looking for the tangency point for a specimen prospective in load control, applying an appropriate stress intensity factor solution for SEB specimen. Fig. 4a reported the crack driving force curve tanget to the experimental cyclic R-curve. Fig.4b presents the R-curve for IN718 at a load ratio of R=0.1. The threshold derived from fitting the El-Haddad model, referred to as $\Delta K_{th,LC}$-adjusted, is lower than the $\Delta K_{th,LC}$ obtained via the CA procedure.

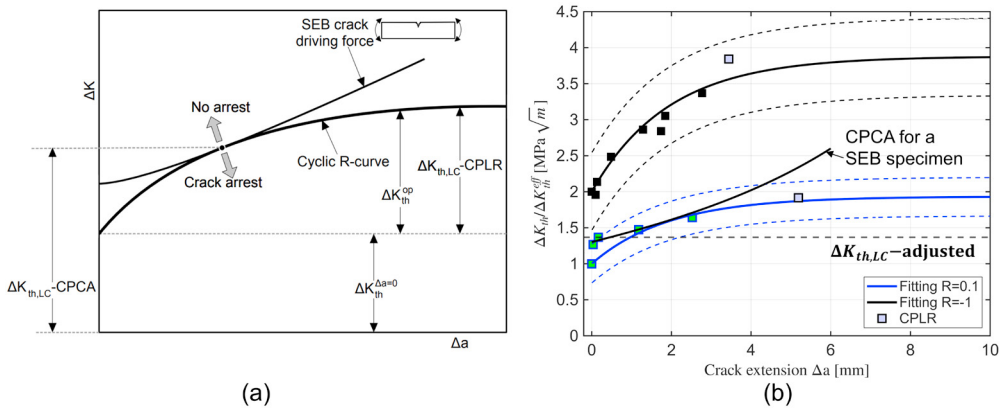

Fig. 4. (a) Definition of long crack threshold based on the R-curve; (b) Experimental cyclic R-curve at the stress ratios R=-1 and 0.1.

3.2.3. Chapetti model

Chapetti (2003) proposed a simplified model to describe the Kitagawa diagram, based on a short crack approach incorporating the cyclic R-curve. The Chapetti model relies on a microstructural threshold defined by the following Eq.4:

$$\Delta K_{th}^{eff} = F \cdot \Delta\sigma_{w,0} \cdot \sqrt{\pi \cdot d} \tag{4}$$

where ΔK_{th}^{eff} represents the starting point of the R-curve and d is the minimum crack size capable of propagation. The parameter d can be expressed as:

$$d = \frac{1}{\pi}\left(\frac{\Delta K_{th}^{\Delta a=0}}{F \cdot \Delta\sigma_{w,0}}\right)^2 \tag{5}$$

Importantly, in the Chapetti model, the material threshold for crack propagation as a function of crack length is directly described by the R-curve reported in Eq.3. In terms of threshold stress, the Chapetti model can be expressed as reported in Eq.6:

$$\Delta\sigma_w = \begin{cases} \dfrac{\Delta K_{\text{th}}^{\Delta a=0} + \left(\Delta K_{\text{th,LC}} - \Delta K_{\text{th}}^{\Delta a=0}\right) \cdot \left[1 - \sum_{i=1}^{n} v_i \cdot \exp\left(-\dfrac{\Delta a}{l_i}\right)\right]}{F \cdot \sqrt{\pi \cdot a}} & \text{if } a \geq d \\ \Delta\sigma_{w,0} & \text{if } a < d \end{cases} \tag{6}$$

To compare the experimental data points, $\Delta\sigma - \sqrt{area}$, of each fatigue series with the El-Haddad and Chapetti models, expressed as functions of crack length, it is necessary to convert $\sqrt{area}$ into an equivalent crack length a_{eq}. The stress intensity factor (SIF) range is $\Delta K = F \cdot \Delta\sigma \cdot \sqrt{\pi \cdot a}$ and it can be expressed using Murakami's parameter to account for irregularly shaped anomalies as Eq.7:

$$\Delta K = Y \cdot \Delta\sigma \cdot \sqrt{\pi \cdot \sqrt{area}} \tag{7}$$

where Y is Murakami's boundary correction factor. The a_{eq} is defined by Eq.8:

$$a_{eq} = \left(\frac{Y}{F}\right)^2 \cdot \sqrt{area} \tag{8}$$

The geometrical factor F follows the Newman and Raju (1981) solution; in this study, all data are referenced to the ISO-K front of the micro-notched specimen, assuming F=0.73.

3.2.4. Fatigue strength models comparison

The experimental results, $\Delta\sigma - a_{eq}$, are compared with the estimated fatigue strength models in Fig.5. A comparison between the El-Haddad and Chapetti models reveals a significant difference in the transition from short to long cracks. In the region corresponding to physically short cracks, the two models define clearly distinct non-propagating domains. Considering the same a_{eq} in this range, the fatigue strength predicted by the R-curve-based Chapetti model is lower than that estimated by the El-Haddad model. This difference is particularly pronounced when using the non-conservative El-Haddad formulation, which is based on larger long-crack threshold value obtained by CPLR procedure. When the El-Haddad model is adjusted through the fitting process (Section 3.2.1), the discrepancy between the two models is reduced, highlighting the influence of threshold selection on fatigue strength predictions.

Fig.5b shows the experimental data points for each of the six 4PB fatigue specimen series, plotted as $\Delta\sigma_w - \sqrt{area}_{average}$. Both the adjusted El-Haddad model and the Chapetti model closely match the experimental results, demonstrating that a single fatigue strength model can effectively predict the behaviour of differently oriented specimen series, with the Chapetti model adds a certain degree of conservatism.

Comparable findings were reported for Co–Cr–Mo alloy in previous works by Romano et al. (2024), where $\sqrt{area}$ estimation based on orientation-dependent roughness parameters, combined with fracture mechanics-based methods, provided a robust assessment; similar conclusions can also be drawn for the IN718 investigated in this study.

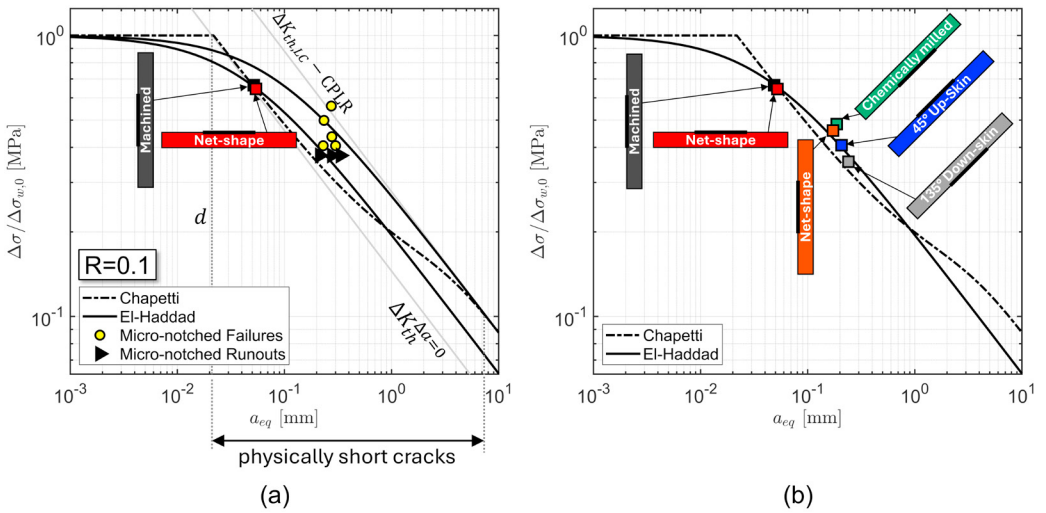

Fig. 5. (a) Kitagawa diagrams (Chapetti, adjusted El-Haddad and El-Haddad adopting $\Delta K_{th,LC}$-CPLR); (b) Kitagawa diagrams compared to the experimental data points of each 4PB fatigue series.

4. Conclusion

The fatigue behaviour of IN718 L-PBF specimens was investigated considering build orientation, surface finishing, and anomalie size. Experimental results were compared with different fatigue strength models, including the El-Haddad and Chapetti approaches. The main conclusions can be summarized as follows:

- Build orientation significantly affects fatigue strength; downskin surfaces show the lowest performance, while horizontal and chemically treated surfaces perform better.
- The El-Haddad model using $\Delta K_{th,LC}$-CPLR procedure overestimates the endurance limit.
- Adjusting the El-Haddad model based on micro-notched specimens provides more accurate fatigue strength predictions that are consistent with the cyclic R-curve.

References

W. E. Frazier, 2014. Metal Additive Manufacturing: A Review. *Journal of Materials Engineering and Performance*, vol. 23, pp. 1917–1928.

E. Hosseini and V. A. Popovich, "A review of mechanical properties of additively manufactured Inconel 718," *Additive Manufacturing*, vol. 30, p. 100877, 2019.

E. Akca and A. Gürsel, "A Review on Superalloys and IN718 Nickel-Based INCONEL Superalloy," *Periodicals of Engineering and Natural Sciences (PEN)*, vol. 3, no. 1, 2015.

N. Sanaei and A. Fatemi, "Defects in additive manufactured metals and their effect on fatigue performance: A state-of-the-art review," *Progress in Materials Science*, vol. 117, p. 100724, 2021.

H. R. Kotadia, G. Gibbons, A. Das, and P. D. Howes, "A review of Laser Powder Bed Fusion Additive Manufacturing of aluminium alloys: Microstructure and properties".

M. Seifi, M. Gorelik, J. Waller, N. Hrabe, N. Shamsaei, S. Daniewicz, and J. J. Lewandowski, "Progress Towards Metal Additive M".

S. R. Daniewicz and N. Shamsaei, "An introduction to the fatigue and fracture behavior of additive manufactured parts," *International Journal of Fatigue*, vol. 94, p. 167, 2017.

S. Romano, A. Brückner-Foit, A. Brandão, J. Gumpinger, T. Ghidini, and S. Beretta, "Fatigue properties of AlSi10Mg obtained".

Y. Yamashita, T. Murakami, R. Mihara, M. Okada, and Y. Murakami, "Defect analysis and fatigue design basis for Ni-based superalloy 718 manufactured by selective laser melting," *International Journal of Fatigue*, vol. 117, pp. 485–495, 2018.

S. Beretta and S. Romano, "A comparison of fatigue strength sensitivity to defects for materials manufactured by AM or traditional processes," *International Journal of Fatigue*, vol. 94, pp. 178–191, 2017.

M. H. El Haddad, K. N. Smith, and T. H. Topper, "Fatigue Crack Propagation of Short Cracks," *Journal of Engineering Materials and Technology*, vol. 101, no. 1, pp. 42–46, Jan. 1979.

M. Chapetti, "Fatigue propagation threshold of short cracks under constant amplitude loading," *International Journal of Fatigue*, vol. 25, pp. 1319–1326, Dec. 2003.

R. Pippan, H. P. Stüwe, and K. Golos, "A comparison of different methods to determine the threshold of fatigue crack propagation," *International Journal of Fatigue*, vol. 16, no. 8, pp. 579–582, 1994.

K. Tanaka and Y. Akiniwa, "Resistance-curve method for predicting propagation threshold of short fatigue cracks at notches," *Engineering Fracture Mechanics*, vol. 30, no. 6, pp. 863–876, 1988.

M. Madia, U. Zerbst, and T. Werner, "Estimation of the Kitagawa-Takahashi diagram by cyclic R curve analysis," *Procedia Structural Integrity*, vol. 38, pp. 309–316, 2022.

D. Perghem, L. Rusnati, L. Patriarca, F. Uriati, and S. Beretta, "Comparison of Fatigue Life and Strength Models for Defective Materials: Application to Scalmalloy in Different Surface Conditions," *Fatigue & Fracture of Engineering Materials & Structures*, vol. 48, no. 7, pp. 3185–3205, 2025.

Y. Murakami, *Metal fatigue: effects of small defects and nonmetallic inclusions*, Academic Press, 2019.

R. Pippan, "The growth of short cracks under cyclic compression," *Fatigue & Fracture of Engineering Materials & Structures*, vol. 9, no. 5, pp. 319–328, 1987.

J. C. Newman and Y. Yamada, "Compression precracking methods to generate near-threshold fatigue-crack-growth-rate data," *International Journal of Fatigue*, vol. 32, no. 6, pp. 879–885, 2010.

A. Pourheidar, L. Patriarca, M. Madia, T. Werner, and S. Beretta, "Progress in the measurement of the cyclic R-curve and its application to fatigue assessment," *Engineering Fracture Mechanics*, vol. 260, p. 108122, Dec. 2021.

L. Patriarca, A. D'Andrea, M. Cova, L. Rusnati, and S. Beretta, "Cyclic R-Curve Measurements for Structural Metallic Alloys," *Advanced Engineering Materials*, vol. 26, no. 19, p. 2400447, 2024.

ASTM E739-21, *Standard Practice for Statistical Analysis of Linear or Linearized Stress-Life (S-N) and Strain-Life (ϵ-N) Fatigue Data*, American Society for Testing And Materials, West Conshohocken, PA, 2023.

K. A. Brownlee, J. L. Hodges, Jr., and M. Rosenblatt, "The Up-and-Down Method with Small Samples," *Journal of the American Statistical Association*, vol. 48, no. 262, pp. 262–277, 1953.

U. Zerbst, M. Madia, and D. Hellmann, "An analytical fracture mechanics model for estimating of S-N curves of metallic alloys containing large second phase particles," *Engineering Fracture Mechanics*, vol. 82, pp. 115–134, 2012.

J. Maierhofer, R. Pippan, and H.-P. Gänser, "Modified NASGRO equation for physically short cracks," *International Journal of Fatigue*, vol. 59, pp. 200–207, 2014.

J. C. Newman and I. S. Raju, "An empirical stress-intensity factor equation for the surface crack," *Engineering Fracture Mechanics*, vol. 15, no. 1, pp. 185–192, 1981.

S. Romano, E. Peradotto, S. Beretta, D. Uguess, L. Barricelli, G. Maculotti, L. Patriarca, and G. Genta, "Fatigue strength estimation of net-shape L-PBF Co–Cr–Mo alloy via non-destructive surface measurements," *International Journal of Fatigue*, vol. 178, p. 108018, 2024.